Earth Planets Space, **62**, 675–684, 2010

Spatial variation in shear wave splitting of the upper crust in the zone of inland high strain rate, central Japan

Yoshihiro Hiramatsu[1], Koichi Iwatsuki[2], Shingo Ueyama[3], Takashi Iidaka[4], and the Japanese University Group of the Joint Seismic Observations at NKTZ

[1]*School of Natural System, College of Science and Engineering, Kanazawa University, Kakuma, Kanazawa, Ishikawa 920-1192, Japan*
[2]*Graduate School of Natural Science and Technology, Kanazawa University, Kakuma, Kanazawa, Ishikawa 920-1192, Japan*
[3]*Department of Earth Sciences, Faculty of Science, Kanazawa University, Kakuma, Kanazawa, Ishikawa 920-1192, Japan*
[4]*Earthquake Research Institute, University of Tokyo, Yayoi 1-1-1, Bunkyo, Tokyo 113-0032, Japan*

(Received March 29, 2010; Revised July 6, 2010; Accepted August 12, 2010; Online published December 13, 2010)

We investigate a detailed spatial variation in shear wave splitting in the zone of inland high strain rate, called the Niigata-Kobe Tectonic Zone (NKTZ), central Japan. Most observations show stress induced anisotropy, that is, the orientation of the faster polarized shear wave is parallel to the axis of the maximum horizontal compressional strain rate estimated from GPS data. Others show structure induced anisotropy, that is, the orientation is parallel to the strike of active faults. For the stress induced anisotropy, time delays normalized by the path length in the anisotropic upper crust is proportional to the differential strain rate. We estimate a spatial variation in stressing rate of the upper crust beneath the high strain rate zone based on a response of the normalized time delay to a step-wise stress change caused by a moderate-sized earthquake. The variation in the stressing rate of 3 kPa/year estimated from shear wave splitting is coincident with that from GPS data. We conclude, together with other seismological features in the NKTZ reported previously, that the high strain rate in the NKTZ is attributed to the high deformation rate below the brittle-ductile transition zone in the crust.

Key words: Shear wave splitting, inland high strain rate zone, Niigata-Kobe Tectonic Zone, stressing rate, spatial variation, brittle-ductile transition zone.

1. Introduction

The accumulation process of stress on faults is one of the most important issues to understand the generation process of earthquakes. A variation in the stress field of the crust controls the distribution of micro-cracks in the crust, causing seismically observable phenomena, such as variations in seismic wave velocity, scattering of seismic wave and anisotropy of seismic wave velocity. Shear wave splitting of natural earthquakes is one of the most powerful tools to investigate the state of the stress in the crust. Shear waves split into two orthogonal wavelets in the anisotropic media, one traveling faster than the other. The preferred alignment of cracks mainly causes the shear wave polarization anisotropy in the upper crust, which is controlled by the differential stress and the pore pressure (Zatsepin and Crampin, 1997). The orientation of the faster polarized shear wave, ϕ, is parallel to the preferred orientation of micro-cracks and is usually consistent with the orientation of a regional maximum horizontal compressional stress (e.g. Kaneshima, 1990). The delay time, δt, or the time difference between two split shear waves, depends on both the aspect ratio and the crack density. Shear wave splitting, therefore, provides information on the state of stress in the crust. In fact, some researchers report that the value of shear wave splitting shows a temporal change due to a stress change before and after an earthquake (e.g. Liu *et al.*, 1997; Hiramatsu *et al.*, 2005) and a volcanic eruption (Miller and Savage, 2001). Recently, Savage *et al.* (2010) reported that a clear correlation between δt and baseline length observed by GPS at Mt. Asama, Japan.

In central Japan, Sagiya *et al.* (2000) reported a concentration zone of high strain rate from Niigata to Kobe, called the Niigata Kobe Tectonic Zone (NKTZ), from a dense network of GPS observation (Fig. 1). The strain rate in the zone is an order of magnitude larger than that of the surrounding areas. As shown in Fig. 1, there are many Quaternary active faults in and around this zone. Some recent large inland earthquakes occurred in and around this zone, the 1995 Hyogo-ken Nanbu earthquake ($M_{\rm JMA}$ 7.3), the 2004 Niigata-ken Chuetsu earthquake ($M_{\rm JMA}$ 6.8), the 2007 Niigata-ken Chuetsu-oki earthquake ($M_{\rm JMA}$ 6.8) and the 2007 Noto Hanto earthquake ($M_{\rm JMA}$ 6.9) (Fig. 1). Furthermore, past large earthquakes seem to concentrate in this zone (Sagiya *et al.*, 2000). This zone is, thus, considered to be a good location to understand the accumulation process of stress in the source region of a large inland earthquake. There are some kinematic models to explain the observed high strain rates in the NKTZ, the detachment model (Hirahara *et al.*, 1998), the collision model (Shimazaki and Zhao, 2000; Heki and Miyazaki, 2001; Miyazaki and Heki, 2001), and the back-slip model (Mazzotti *et al.*, 2000). Iio *et al.* (2002), however, rejected all of the models by consid-

doi:10.5047/eps.2010.08.003

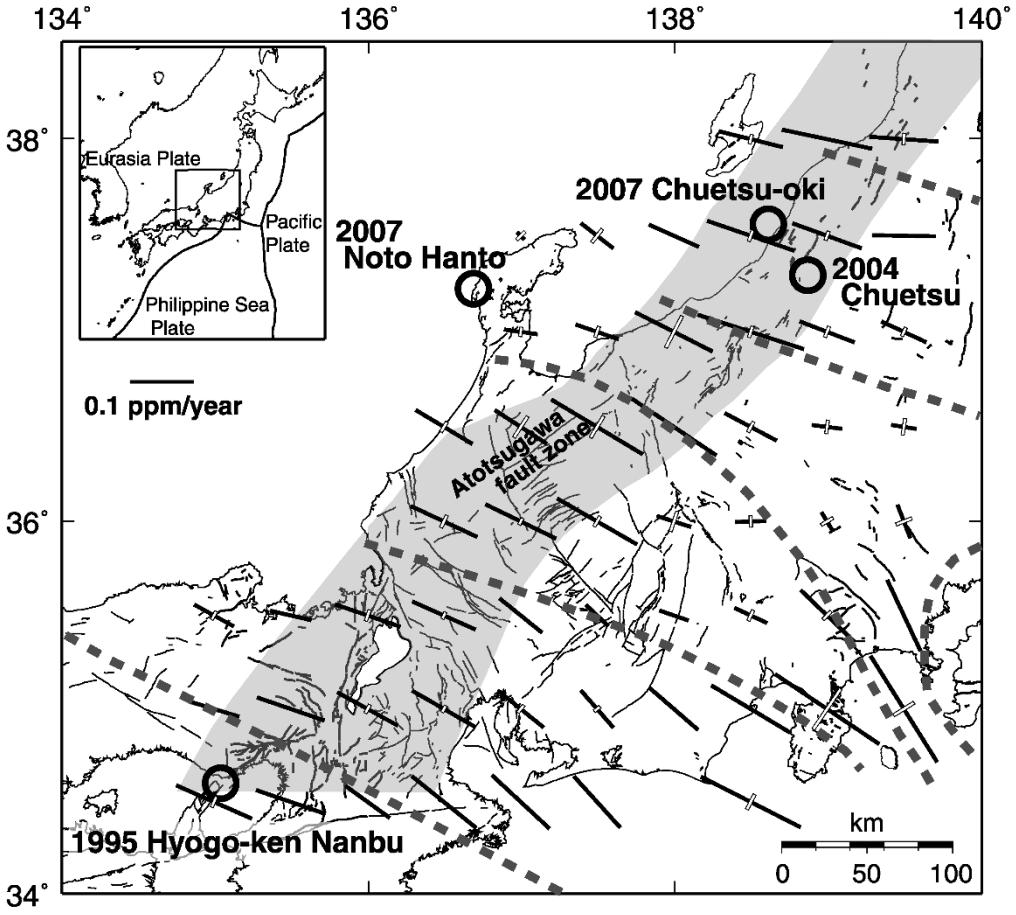

Fig. 1. Distribution of the principal strain rate axes (black bars: compression, white bars: extension), the high strain rate zone called the Niigata-Kobe Tectonic Zone (gray zone) (Sagiya *et al*., 2000), the trajectories of the maximum horizontal compressional stress (Ando, 1979) (gray dashed lines), Quaternary active faults (lines), and recent large earthquakes in and around the high strain rate zone (circles).

ering the physical validity on these models based on stress field, mantle flow and fault movement in the high strain rate zone. Instead, Iio *et al*. (2002, 2004) proposed the weak zone model that has a weak zone with lower viscosity in the lower crust beneath the NKTZ. Smaller strength in the crust is, thus, expected to deform at a higher strain rate in their model.

Seismic structure from the crust to the upper mantle is an important point to understand the origin of the high strain rate zone. Tomographic studies revealed the existence of a low velocity zone in the lower crust (Nakajima and Hasegawa, 2007a; Matsubara *et al*., 2008) and in the mantle wedge (Nakajima and Hasegawa, 2007b) beneath the NKTZ. A distinct anisotropic body is observed from shear wave splitting in the mantle wedge beneath the central part of the NKTZ (Hiramatsu *et al*., 1998). Jin and Aki (2005) reported that the NKTZ is characterized by low coda Q, lower than 90 for 1–2 Hz and lower than 170 for 2–4 Hz. The Japanese University Group of the Joint Seismic Observations at NKTZ started seismic observations around the Atotsugawa fault zone, north central Japan, from 2004 (The Japanese University Group of the Joint Seismic Observations at NKTZ, 2005). Iidaka *et al*. (2009) confirmed strong anisotropy in the mantle wedge beneath the NKTZ from many shear wave splitting data obtained by this dense network.

In and around the NKTZ, the principal stress axes are coincident with the principal strain rate axes (Fig. 1). This feature shows that the high strain rate at the surface reflects directly the state of stress in the crust. Shear wave splitting, thus, provides useful information to reveal the cause of the high strain rate zone. We report here a spatial distribution of shear wave splitting in and around the NKTZ to investigate the stress condition in the upper crust and show that shear wave splitting is controlled by the strain rate. From this result, together with a temporal change in time delay due to a step-wise stress change caused by a moderate-sized earthquake (Hiramatsu *et al*., 2005), we estimate a spatial variation in stressing rate of the upper crust beneath the NKTZ and conclude that the high strain rate in the NKTZ is attributed to the high deformation rate below the brittle-ductile transition zone in the crust.

2. Data and Method

We use seismic waveform data recorded at stations of the Japanese university joint seismic observations at NKTZ, Earthquake Research Institute, University of Tokyo, Disaster Prevention Research Institute, Kyoto University, Research Center for Seismology, Volcanology and Disaster Mitigation, Nagoya University, Japan Meteorological Agency (JMA), Geological Survey of Japan (GSJ), and Hi-net data operated by the National Research Institute for

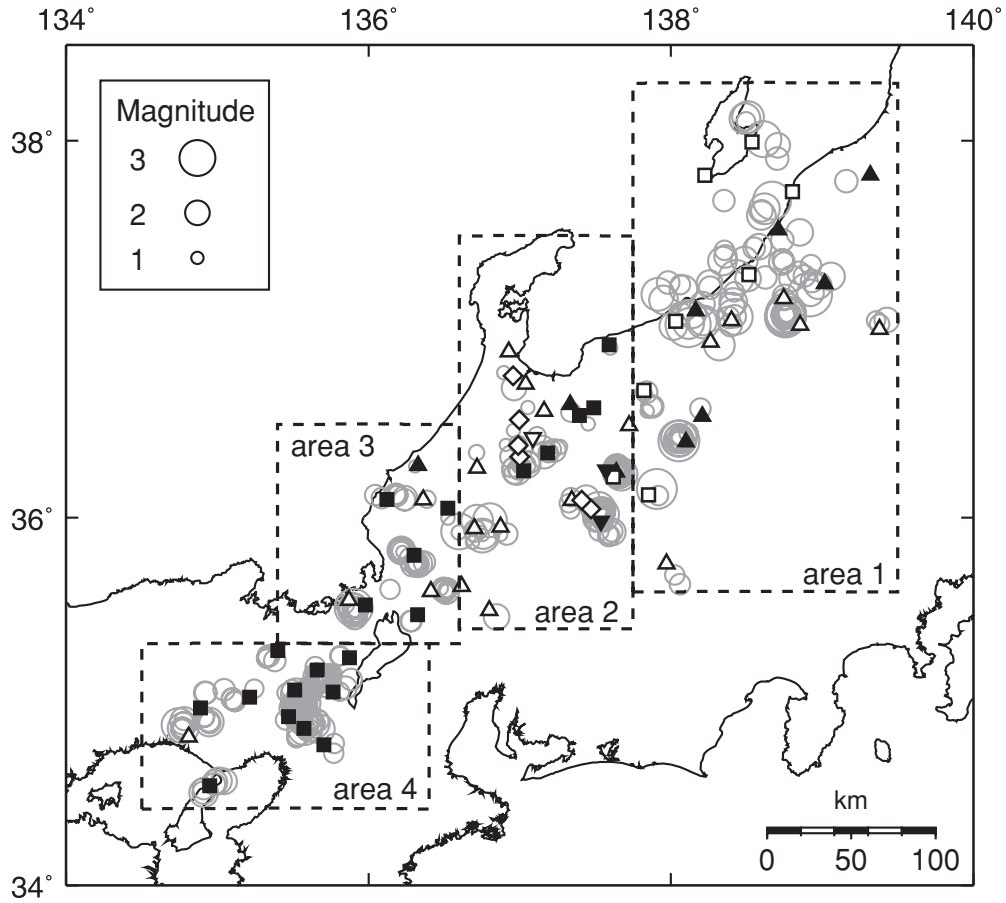

Fig. 2. Events (circles) and stations (open squares: Univ. of Tokyo, solid squares: Kyoto Univ., open triangles: NIED, solid triangles: JMA, open inverse triangles: GSJ, solid inverse triangles: Nagoya Univ., Diamonds: The Japanese University Group of the Joint Seismic Observations at NKTZ) used in this study. Dashed rectangles show areas where we adopt different velocity models in Fig. 3.

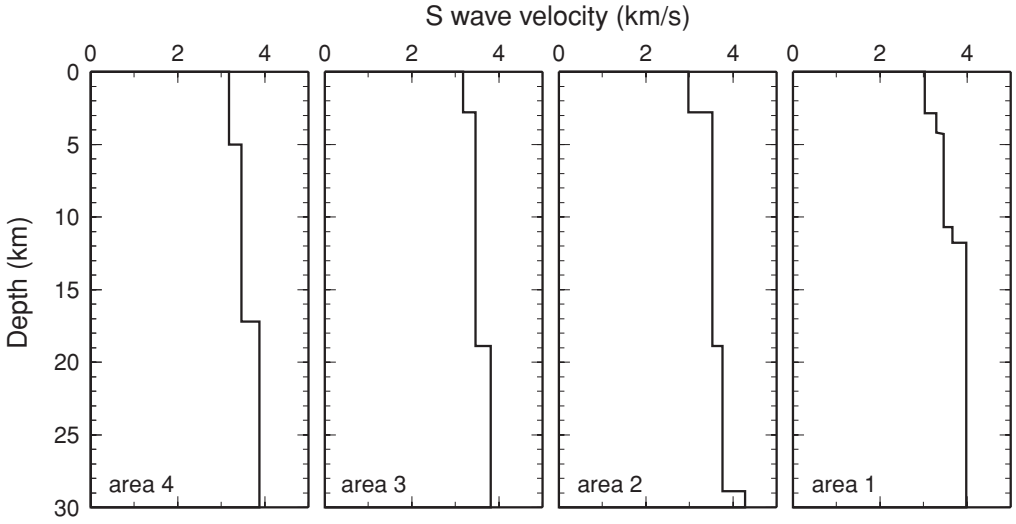

Fig. 3. S wave velocity model of each area. S waves velocity is given by P waves velocity with a relationship $V_P/V_S = 1.73$.

Earth Science and Disaster Prevention (NIED), in central Japan (Fig. 2). The period of the analysis covers mainly the years from 1998 to 2002 for all stations except those of the Japanese university joint seismic observations at NKTZ. For the stations around the Atotsugawa fault zone (in area 2 in Fig. 2), in particular the stations of the Japanese university joint seismic observations at NKTZ, the analyzed period covers form October 2004 to the end of 2006.

We analyze waveform data that satisfy the following conditions. Source depths are restricted within 30 km to investigate crustal anisotropy. Incident angles are less than 35° to minimize the effect of phase conversion from S to P or the distortion of particle motions at the free surface (Booth and Crampin, 1985). For the calculation of ray path from

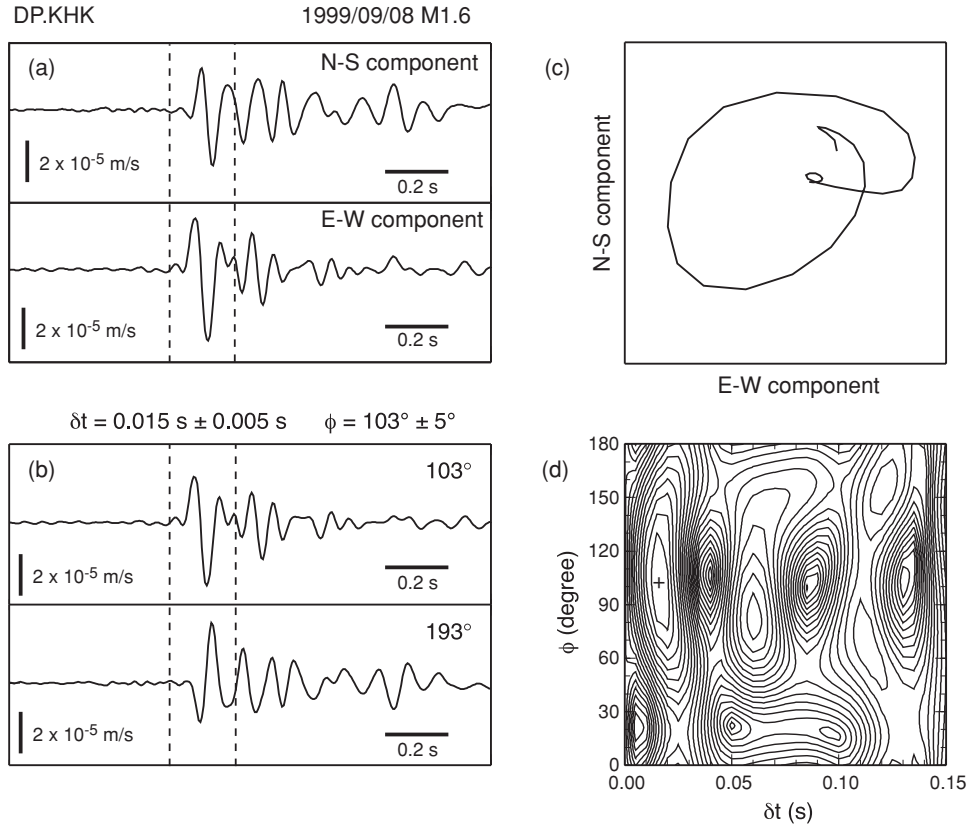

Fig. 4. An example of waveform data and splitting analysis at station DP.KHK. (a) Original waveforms of band-pass filtered two horizontal components. Dashed lines show the time window for particle motion and splitting analysis. (b) Particle motion of two horizontal components. (c) Rotated waveforms of faster shear wave (upper) and slower one (lower). (d) Contour map of the confidence level by the method of Silver and Chan (1991). Plus shows the optimum splitting parameters of δt and ϕ. A contour interval corresponds to the confidence level of two times of the standard error.

a source to a station and incident angle, we divide the analyzed region into four areas depending on the velocity structure used for the hypocenter determination of local events (Tsukuda *et al.*, 1992; Ito *et al.*, 1995) (Fig. 2 and Fig. 3). We usually use events whose magnitudes are larger than 1.5 to certify high signal to noise ratios and clear *S* waveforms. However, we use some events whose magnitudes are larger than 1.0 if those waveforms are clear enough to obtain the splitting parameters. The sampling frequency of waveform data differs with stations, mainly 100 Hz, 80 Hz and 200 Hz. We estimate the splitting parameters, ϕ and δt, using the covariance matrix decomposition method of Silver and Chan (1991) from the band-pass filtered (1–20 Hz) two horizontal components of *S* waves (Fig. 4). We also confirm visually that the obtained splitting parameters are coincident with the initial motion of *S* waves from the particle motion. Finally, we obtain a total of 501 shear wave splitting measurements at 67 stations from 477 events (Fig. 2 and Fig. 5).

3. Spatial Variations in the Splitting Parameters in and around the NKTZ

We show all splitting parameters obtained in this study in Fig. 5. Most of ϕ show the orientation of NW-SE or WNW-ESE and are parallel to the axis of maximum horizontal compression stress as reported by Ando (1979) or the axis of maximum horizontal compression strain rate estimated from continuous GPS data (Sagiya *et al.*, 2000) as shown in Fig. 1, indicating stress induced anisotropy. Noting around the Atotsugawa fault zone, our result is consistent with a recent regional study of shear wave splitting (Mizuno *et al.*, 2005). However, some stations, especially in area 1, show that ϕ is not coincident with the axes of the stress or the strain rate but the strike of active faults and folds around the stations, indicating structure induced anisotropy. Figure 6 shows the depth distribution of δt in each area. The observed δt reaches mainly up to 0.1 s, which is typical value of crustal anisotropy. It seems that the δt is likely to be proportional to the source depth up to 10–15 km and seems not to be proportional past the depth of 15 km, suggesting the anisotropic layer is restricted in the upper $\sim$15 km depth. To discuss the strength of crustal anisotropy, it is preferable that we do not use time delay, δt, but time delay normalized by path length in the anisotropic layer, δt_n. Considering the depth variations of δt and event number, we assume that the anisotropic layer is upper 15 km in the crust in areas 1, 3 and 4 and upper 12 km in area 2 although the depth variation of δt may not be so clear in areas 1 and 2. A considerable uncertainty of the thickness of the anisotropic layers, about 1–2 km, has little effect on the following discussion. Hereafter, we use the average value of the normalized time delay at each station to show the strength of the crustal anisotropy as well as ϕ.

We show the spatial distribution of the average orientation of ϕ and the average normalized time delay at each station in Fig. 7. Here, we consider that the anisotropy is the stress induced anisotropy when the angular differ-

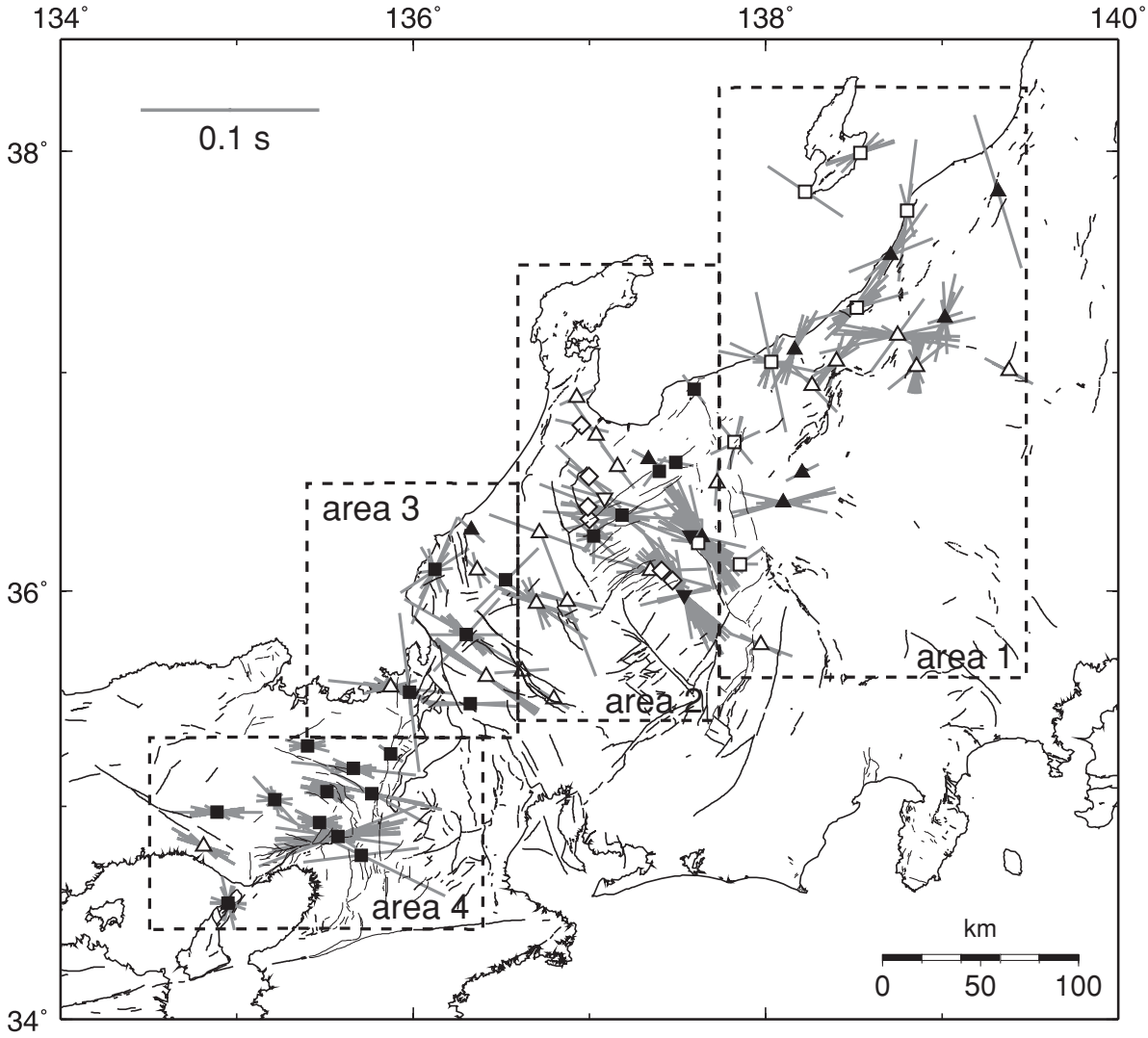

Fig. 5. Results of shear wave splitting at each station. The orientation and the length of each bar show the orientation of faster shear waves and the time delay between two split shear waves. Lines are Quaternary active faults.

ence between the average ϕ and the principal compressional axis of the strain rate is within 30°. Otherwise, we treat the anisotropy as the structure induced anisotropy. This map confirms again that most stations in areas 2, 3, and 4 show stress induced anisotropy (black and dark gray bars in Fig. 7) and most stations in area 1 show structure induced anisotropy (light gray bars in Fig. 7). Area 1 is characterized by a thick, 6 km thickness, Miocene–Pleistocene sedimentary basin where NNE-SSW trended faults and folds are developed actively (Yanagisawa *et al.*, 1986). Such a thick sedimentary basin was confirmed also by a seismic tomography (Kato *et al.*, 2006). A high activity of faulting and folding in the sedimentary basin may generate more easily the structure induced anisotropy rather than the other areas, suggesting less stress induced anisotropy in area 1. The normalized time delay ranges mainly from 1 to 6 ms/km and shows large values in area 2. To investigate the relationship between the strength of crustal anisotropy and the strain rate, we focus on the stations whose angular difference between the average ϕ and the orientation of the principal compressional axis of the strain rate is within 30° and the data number is greater than or equal to 3 (black bars in Fig. 7).

Figure 8 shows the relationship between the normalized time delay and the differential strain rate estimated from the GPS data (Sagiya *et al.*, 2000). The differential strain rate is calculated by subtracting the strain rate of the compressional axis from that of the extensional axis because this differential strain rate acts to open the micro-cracks aligned parallel to the principal compressional axis of the strain rate. We recognize a positive correlation between the normalized time delay and the differential strain rate. In general, the strength of the anisotropy in the upper crust is interpreted by the strength of the crustal stress. This positive correlation, however, indicates that the strength of the stress induced anisotropy is controlled by the strain rate, in other words, the stressing rate in the crust as well.

4. A Variation in the Stressing Rate in the NKTZ Estimated from Shear Wave Splitting

Here we estimate a variation in the stressing rate in the NKTZ from the spatial variation in the normalized time delay of shear wave splitting. Hiramatsu *et al.* (2005) reported that the increase in time delay induced by the static stress

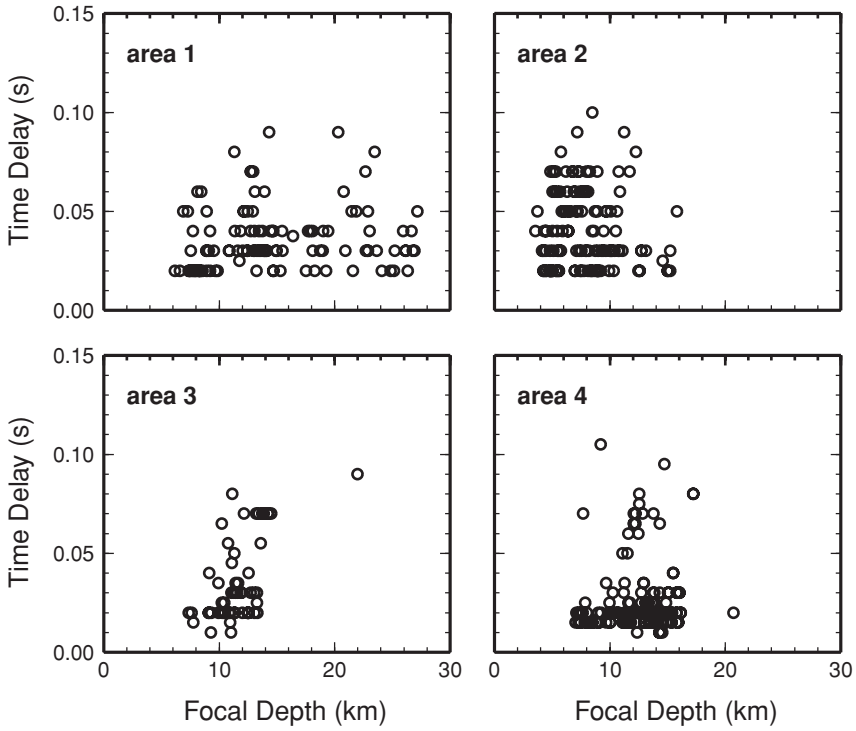

Fig. 6. Plots of depth versus time delay of two split shear waves in each area.

change due to a moderate size earthquake recovered to the pre-event value within about two years from the observation of shear wave splitting. This means that a variation in the condition of micro-cracks due to a step-wise stress change recovers to a steady state within about two years. The balance between the opening of micro-cracks due to a constant stressing rate and the rate of the healing of micro-cracks determines the steady state crack condition. As proposed by Hiramatsu *et al*. (2005), the time constant of the healing of cracks is universally constant. Thus, the normalized time delay is expected to be a function of the stressing rate. The proportional relationship between the normalized time delay and the differential strain rate supports the proposition by Hiramatsu *et al*. (2005). The observed variation in the normalized time delay can, therefore, be interpreted to reflect the variation in the stressing rate in the NKTZ.

To estimate the variation in the stressing rate from shear wave splitting, we use RSC_{SP}, the response of normalized time delay per unit stress change, as follows,

$$\mathrm{RSC}_{SP} = \frac{1}{\Delta\sigma}\frac{\Delta\delta t_n}{\delta t_n} \tag{1}$$

where $\Delta\sigma$ is the static stress change and $\Delta\delta t_n/\delta t_n$ the fractional change of the normalized time delay. The results of the temporal change in the normalized time delay due to the static stress change by the Aichi-ken Tobu earthquake (Saiga *et al*., 2003; Hiramatsu *et al*., 2005) provides δt_n of 1.6 ms/km as the steady state value and $\Delta\delta t_n$ of 1.4 ms/km as the increase of the normalized time delay due to $\Delta\sigma$ of 1.0 kPa as the increase of the effective static stress for opening or enlargement of micro-cracks. Based on these values, RSC_{SP} is estimated to be 880 $(\mathrm{MPa})^{-1}$. Applying the value of RSC_{SP} estimated from the temporal change to the case of a spatial variation in stress, the spatial variation in the stressing rate is defined as,

$$\dot{\sigma} = \frac{1}{\mathrm{RSC}_{SP}}\frac{\Delta\delta t_n}{\delta t_n}\frac{1}{T_C} \tag{2}$$

where $\dot{\sigma}$ is the spatial variation in the stressing rate, $\Delta\delta t_n/\delta t_n$ the fractional change of the normalized time delay in a region of interest, and T_C the time constant. This formulation can be interpreted that a constant stressing rate is approximated by a successive step-wise stress change with a constant time interval T_C. The value of $\Delta\delta t_n/\delta t_n$ is estimated to be 5.5 in this study using a linear trend between the differential strain rate and the normalized time delay (Fig. 8) because higher strain rates correspond to the inner zone of the NKTZ and lower ones to the outer zone. We apply two years as T_C (Hiramatsu *et al*., 2005). Substituting these values into Eq. (2), we can estimate the variation in the stressing rate in the NKTZ as 3±0.6 kPa/year. Assuming the rigidity of 40 GPa, we obtain the variation in the stressing rate is about 3 kPa/year in the NKTZ from the strain rate estimated from GPS observation shown in Fig. 1. We calculate here the variation in stressing rate as 0.5×rigidity×(a variation in differential strain rate), that is, the variation in stressing rate of shear stress. This value is coincident with that estimated from shear wave splitting data. The variation in the stressing rate estimated from shear wave splitting represents the average one in the brittle upper crust. We can, thus, regard the variation in the stressing rate at surface estimated from GPS data as that in the brittle upper crust.

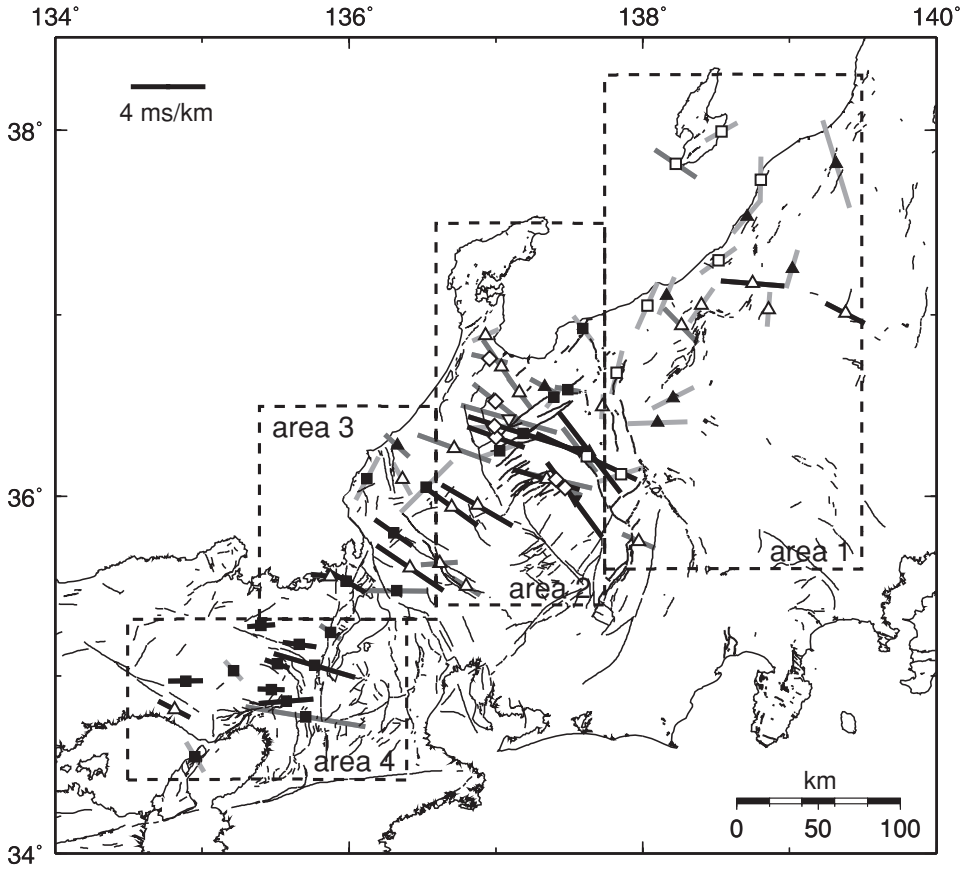

Fig. 7. The average orientation of faster shear waves and the average time delay normalize by path lengths in anisotropic upper crust. Black bars show that the angular difference between the average orientation and the orientation of the principal compressional axis of the strain rate is within 30° and the data number is greater than or equal to 3 that are used for the plot of Fig. 8. Dark gray bars indicate that the angular difference is within 30° and the data number is smaller than or equal to 2 and light gray bars indicate that the angular difference is greater than 30°. Lines are Quaternary active faults.

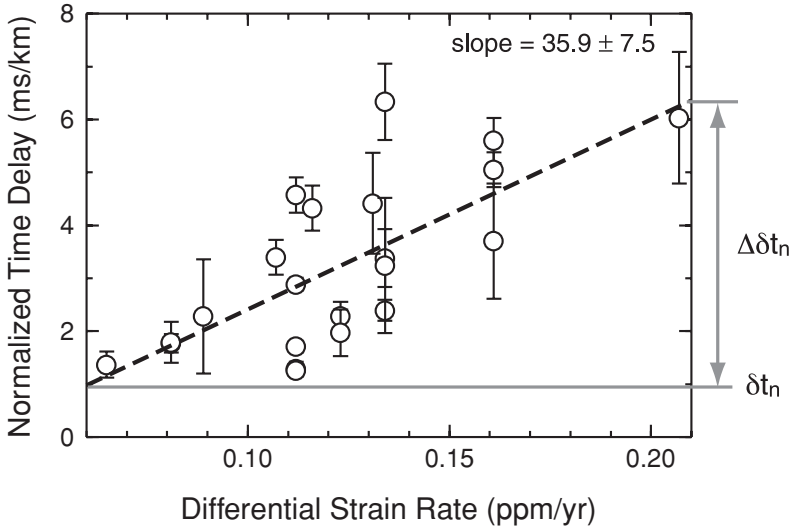

Fig. 8. Plot of the differential strain rate observed by GPS (Sagiya *et al.*, 2000) versus the average normalized time delay at stations whose angular difference between the average orientation of faster shear waves and the orientation of the principal compression axis of the strain rate is within 30° and the data number is greater than or equal to 3 that are shown by black bars in Fig. 7. The dashed line is the least squares fit to the data (normalized time delay (ms/km) $= -1.2 + 35.9 \times$ differential strain rate (ppm/yr)). Gray lines represent the definition of δt_n and $\Delta\delta t_n$ in Eq. (2).

5. Discussion

We estimate the variation in the stressing rate of 3±0.6 kPa/year in the NKTZ from the results of shear wave splitting. The variation deduced from shear wave splitting is considered to reflect that in the brittle upper crust. To discuss a cause of the concentration of high strain rate in the NKTZ, this information is insufficient because a previous model stressed an importance of the role of ductile lower

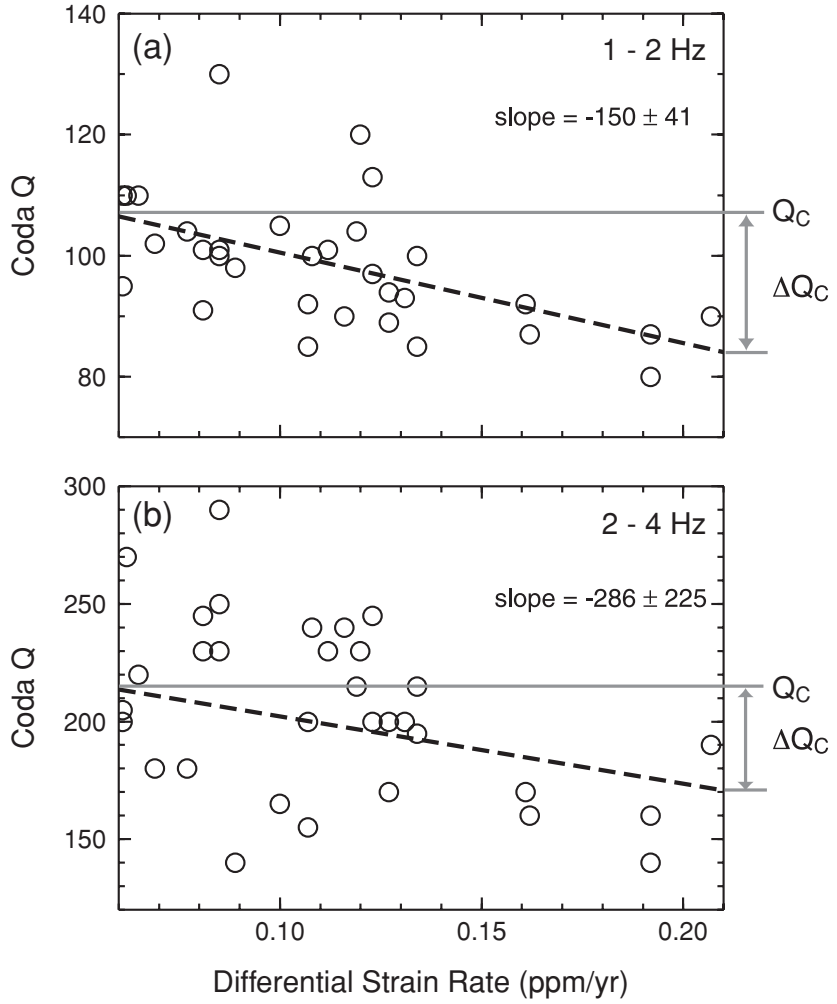

Fig. 9. Plots of the differential strain rate observed by GPS (Sagiya *et al*., 2000) versus the coda Q of (a) 1–2 Hz and (b) 3–4 Hz reported by Jin and Aki (2005). Dashed line is the least squares fit to the data. Gray lines and an arrow represent the definition of Q_C and ΔQ_C in Eq. (3).

crust (Iio *et al*., 2002, 2004). Seismic tomography studies also showed that the NKTZ was characterized by low velocity zones in the lower crust (Nakajima and Hasegawa, 2007a; Matsubara *et al*., 2008). One of the possible tools to infer the stress state in the ductile lower crust is coda Q because coda waves sample the whole crust and are considered to be a good indicator of the stress state in the crust (Aki, 1980; Hiramatsu *et al*., 2000). It is, thus, interesting to discuss the spatial variation in the stressing rate in the NKTZ using results of a spatial variation and a temporal variation in coda Q of previous studies.

Jin and Aki (2005) showed that the NKTZ was characterized by low coda Q, lower than 90 for 1–2 Hz and lower than 170 for 2–4 Hz. Hiramatsu *et al*. (2000) reported a temporal variation in the coda Q in the Tamba region that is included in the NKTZ due to the static stress change induced by the 1995 Hyogo-ken Nanbu earthquake only at frequency bands lower than 4 Hz. They estimated the response of coda Q per unit stress change (RSC_{Q_C}) of 10 $(\mathrm{MPa})^{-1}$ at lower frequencies. Sugaya *et al*. (2009) analyzed a temporal variation in coda Q in the Tamba region following the period of Hiramatsu *et al*. (2000). They confirmed that the value of coda Q recovered to the pre-event value within two years at lower frequencies. This suggests that a modification of crack condition due to a step-wise stress change recovers to a steady state within about two years as well as the case of shear wave splitting. If we apply the same approach mentioned in the previous section, the spatial variation in coda Q at 1–2 Hz and 2–4 Hz frequency bands in and around the NKTZ reported by Jin and Aki (2005) can be interpreted to reflect the variation in the stressing rate in the crust.

We, thus, estimate a spatial variation in stressing rate in the analyzed region, $\dot{\sigma}$, from coda Q as follows,

$$\dot{\sigma} = \frac{1}{\mathrm{RSC}_{Q_C}} \frac{\Delta Q_C}{Q_C} \frac{1}{T_C} \tag{3}$$

where $\Delta Q_C / Q_C$ is the fraction of the spatial variations in coda Q. We adopt $\mathrm{RSC}_{Q_C} = 10$ $(\mathrm{MPa})^{-1}$ based on the temporal change in the coda Q at lower frequencies in the Tamba region (Hiramatsu *et al*., 2000) and $T_C = 2$ years in the same way as the shear wave splitting. To evaluate $\Delta Q_C / Q_C$, we use a linear trend between the coda Q (Jin and Aki, 2005) and the differential strain rate in and around the NKTZ (Sagiya *et al*., 2000) (Fig. 9). We can find a negative correlation between the coda Q and the differential strain rate for both frequency bands. Following the measurement of $\Delta Q_C / Q_C$ of Hiramatsu *et al*. (2000),

we define ΔQ_C and Q_C as shown in Fig. 9, providing $\Delta Q_C/Q_C = 0.26$ at 1–2 Hz and $\Delta Q_C/Q_C = 0.27$ at 2–4 Hz. Substituting these values into Eq. (3), we estimate the variation in the stressing rate of about 13±3.5 kPa/year for 1–2 Hz frequency band and about 13±10 kPa/year for 2–4 Hz frequency band in the analyzed region. The variation in the stressing rate estimated from coda Q of 1–2 Hz frequency band is, thus, larger obviously than that from GPS or shear wave splitting. The variation in the stressing rate estimated from coda Q of 3–4 Hz frequency band also provides a larger stressing rate than that from GPS or shear wave splitting. However, a large error obscures its significance for 3–4 Hz frequency band.

One of the keys to solve this discrepancy of the variation in the stressing rate is to examine what the variation in coda Q reflects. Jin and Aki (1989) proposed the creep model in which coda Q was a parameter that reflects the degree of creep in the ductile part of the crust. Sugaya *et al.* (2009) also concluded that the variation in coda Q reflected possibly a change in the ductile fracture in the brittle-ductile transition zone in the crust from studies of the temporal variations in coda Q and seismicity. A spatial correlation between the low coda Q zone (Jin and Aki, 2005) and the low velocity zone in the lower crust from seismic tomography (Nakajima and Hasegawa, 2007a; Matsubara *et al.*, 2008) in NKTZ also suggests that the coda Q at 1–2 Hz and 2–4 Hz frequency bands is related to a scattering property in the lower crust primarily. These studies suggest that the variation in the stressing rate estimated from coda Q at 1–2 Hz and 2–4 Hz frequency bands is caused by a variation in the ductile deformation rate below the brittle-ductile transition zone in the crust.

We, thus, interpret that the discrepancy between the variations in the stressing rate estimated from shear wave splitting and from coda Q reflects the difference of the variation in stressing rate between the brittle upper crust and the ductile part below the brittle-ductile transition zone in the crust. From this point of view, we prefer the weak zone model (Iio *et al.*, 2002) as the cause of the NKTZ. The weak zone model explains the high strain rate in terms of deformations in a weak zone with lower viscosity in the lower crust beneath the NKTZ. The high deformation rate inferred from the high stressing rate from coda Q possibly suggests that a weak zone is formed by ductile fractures as argued by Jin and Aki (2005).

Finally, we mention a precursory change in shear wave splitting on earthquake. Several researchers reported an increase of time delay before earthquakes (e.g. Crampin *et al.*, 1999) although it has been controversial. This kind of increase is usually interpreted to be caused by the increase or the enlargement in micro-cracks due to the increase of regional tectonic or local differential stress around the source fault. Some numerical simulations based on the constitutive law of the friction, such as rate- and state-dependent friction law (Dieterich, 1979), show an accelerated slip on the nucleation region of a source fault before earthquake (e.g. Kato, 2004). This accelerated slip generates the increase in the strain rate or stressing rate around the source fault, causing the temporal variation in the differential stress. As shown in this study, the time delay of shear wave splitting is sensitive to the differential strain rate or stressing rate. Shear wave splitting may, therefore, detect a variation in the stressing rate due to the accelerated slip on the nucleation region if proper data set is available.

6. Conclusions

To understand the state of the stress in the high strain rate zone, called the NKTZ, and the cause of the NKTZ, we investigate a detailed spatial variation in shear wave splitting in the crust using waveform data at dense seismic stations. We find that the orientation of the faster polarized shear wave is parallel to the axis of the maximum horizontal compressional strain rate estimated from GPS data at most stations. We call this type as the stress induced anisotropy because the principal axes of the strain rate coincides with those of the horizontal stress in the analyzed region. On the other hand, the orientation of the faster polarized shear wave is parallel to the strike of active faults at some stations, indicating the structure induced anisotropy. A proportional relationship between the time delays normalized by the path length in the anisotropic upper crust and the differential strain rate confirms that the strength of the crustal anisotropy is controlled by the strain rate or the stressing rate. A spatial variation in stressing rate of the upper crust beneath the NKTZ is estimated using a response of the normalized time delay to a step-wise stress change caused by a moderate-sized earthquake. The variation in stressing rate estimated from shear wave splitting is 3 kPa/year. This value is coincident with a corresponding stressing rate of 3 kPa/year estimated from GPS data. Stressing rate estimated from coda Q and seismological features in the NKTZ indicate that the ductile fractures below the brittle-ductile transition zone can cause high deformation rate in the crust, resulting in the high strain rate at surface of the NKTZ.

Acknowledgments. We thank the National Research Institute for Earth Science and Disaster Prevention, Japan Meteorological Agency, Geological Survey of Japan, Earthquake Research Institute, University of Tokyo, Disaster Prevention Research Institute, Kyoto University, and Research Center for Seismology, Volcanology and Disaster Mitigation, Nagoya University for providing the waveform data collected at online stations. Comments from anonymous reviewers are useful to improve the manuscript. All figures are made using the GMT software (Wessel and Smith, 1998). This research was partly supported by a grant offered under the Earthquake Prediction Research program of the Ministry of Education, Culture, Sports, Science and Technology of Japan.

References

Aki, K., Scattering and attenuation of shear waves in the lithosphere, *J. Geophys. Res.*, **85**, 6496–6504, 1980.

Ando, M., The stress field of the Japanese Islands in the last 0.5 million years, *Earth Mon. Symp.*, **7**, 541–546, 1979 (in Japanese).

Booth, D. C. and S. Crampin, Shear-wave polarizations on a curved wavefront at anisotropic free surface, *Geophys. J. R. Astron. Soc.*, **83**, 31–45, 1985.

Crampin, S., T. Volti, and R. Stefansson, A successfully stress-forecast earthquake, *Geophys. J. Int.*, **138**, F1–F5, 1999.

Dieterich, J. H., Modeling of rock friction 1. Experimental results and constitutive equations, *J. Geophys. Res.*, **84**, 2161–2168, 1979.

Heki, K. and S. Miyazaki, Plate convergence and long-term crustal deformation, *Geophys. Res. Lett.*, **28**, 2313–2316, 2001.

Hirahara, K., M. Ando, Y. Hoso, Y. Wada, and T. Nakano, Search for the movement of an active fault by GPS measurements, *Earth Mon.*, **225**, 149–153, 1998 (in Japanese).

Hiramatsu, Y., M. Ando, T. Tsukuda, and T. Ooida, Three-dimensional image of the anisotropic bodies beneath central Honshu, Japan, *Geophys. J. Int.*, **135**, 801–816, 1998.

Hiramatsu, Y., N. Hayashi, M. Furumoto, and H. Katao, Temporal changes in coda Q^{-1} and b-value due to the static stress change associated with the 1995 Hyogo-ken Nanbu earthquake, *J. Geophys. Res.*, **105**, 6141–6151, 2000.

Hiramatsu, Y., H. Honma, A. Saiga, M. Furumoto, and T. Ooida, Seismological evidence on characteristic time of crack healing in the shallow crust, *Geophys. Res. Lett.*, **32**, L09304, doi:10.1029/2005GL022657, 2005.

Iidaka, T., Y. Hiramatsu, and The Japanese University Group of the Joint Seismic Observations at NKTZ, Shear-wave splitting analysis of the upper mantle at the Niigata-Kobe Tectonic Zone with the data of the Joint Seismic Observations at NKTZ, *Earth Planets Space*, **61**, 227–235, 2009.

Iio, Y., T. Sagiya, Y. Kobayashi, and I. Shiozaki, Water-weakened lower crust and its role in the concentrated deformation in the Japanese Islands, *Earth Planet. Sci. Lett.*, **203**, 245–253, 2002.

Iio, Y., T. Sagiya, and Y. Kobayashi, Origin of the concentrated deformation zone in the Japanese Islands and stress accumulation process of intraplate earthquake, *Earth Planets Space*, **56**, 831–842, 2004.

Ito, K., K. Matsumura, H. Wada, N. Hirano, S. Nakao, T. Shibutani, K. Nishigami, H. Katao, F. Takeuchi, K. Watanabe, H. Watanabe, and H. Negishi, Seismological layer of the crust in the inner zone of southwest Japan, *Annuals, Disas. Prev. Res. Inst., Kyoto Univ.*, **38**, 209–219, 1995 (in Japanese with English abstract).

Jin, A. and K. Aki, Spatial and temporal correlation between coda Q^{-1} and seismicity and its physical mechanism, *J. Geophys. Res.*, **94**, 14041–14059, 1989.

Jin, A. and K. Aki, High-resolution maps of coda Q in Japan and their interpretation by the brittle-ductile interaction hypothesis, *Earth Planets Space*, **57**, 403–409, 2005.

Kaneshima, S., Origin of crustal anisotropy: shear wave splitting studies in Japan, *J. Geophys. Res.*, **97**, 11121–11133, 1990.

Kato, A., S. Sakai, N. Hirata, E. Kurashimo, T. Iidaka, T. Iwasaki, and T. Kanazawa, Imaging the seismic structure and stress field in the source region of the 2004 mid-Niigata prefecture earthquake: Structural zones of weakness and seismogenic stress concentration by ductile flow, *J. Geophys. Res.*, **111**, B08308, doi:10.1029/2005JB004016, 2006.

Kato, N., Interaction of slip on asperities: Numerical simulation of seismic cycles on a two-dimensional planar fault with nonuniform frictional property, *J. Geophys. Res.*, **109**, B12306, doi:10.1029/2004JB003001, 2004.

Liu, Y., S. Crampin, and I. Main, Shear-wave anisotropy: spatial and temporal variations in time delays at Parkfield, Central California, *Geophys. J. Int.*, **130**, 771–785, 1997.

Matsubara, M., K. Obara, and K. Kasahara, Three-dimensional P- and S-wave velocity structures beneath the Japanese Islands obtained by high-density seismic stations by seismic tomography, *Tectonophysics*, **454**, 86–103, 2008.

Mazzotti, S., X. Le Pichon, and P. Henry, Full interseismic locking of the Nankai and Japan-west Kurile subduction zones: An analysis of uniform elastic strain accumulation in Japan constrained by permanent GPS, *J. Geophys. Res.*, **105**, 13159–13177, 2000.

Miller, V. and M. Savage, Changes in seismic anisotropy after volcanic eruptions: evidence from Mount Ruapehu, *Science*, **293**, 2231–2233, 2001.

Miyazaki, S. and K. Heki, Crustal velocity field of southwest Japan: Subduction and arc-arc collision, *J. Geophys. Res.*, **106**, 4305–4326, 2001.

Mizuno, T., H. Ito, Y. Kuwahara, K. Imanishi, and T. Takeda, Spatial variation of shear-wave splitting across an active fault and its implication for stress accumulation mechanism of inland earthquakes: The Atotsugawa fault case, *Geophys. Res. Lett.*, **32**, L20305, doi:10.1029/2005GL023875, 2005.

Nakajima, J. and A. Hasegawa, Deep crustal structure along the Niigata-Kobe Tectonic Zone, Japan: Its origin and segmentation, *Earth Planets Space*, **59**, e5–e8, 2007a.

Nakajima, J. and A. Hasegawa, Subduction of the Philippine Sea plate beneath southwestern Japan: Slab geometry and its relationship to arc magmatism, *J. Geophys. Res.*, **112**, B08306, doi:10.1029/2006JB004770, 2007b.

Sagiya, T., S. Miyazaki, and T. Tada, Continuous GPS array and present-day crustal deformation of Japan, *Pure Appl. Geophys.*, **157**, 2003–2322, 2000.

Saiga, A., Y. Hiramatsu, T. Ooida, and K. Yamaoka, Spatial variation in the crustal anisotropy and its temporal variation associated with the moderate size earthquake in the Tokai region, central Japan, *Geophys. J. Int.*, **154**, 695–705, 2003.

Savage, M. K., T. Ohminato, Y. Aoki, H. Tsuji, and S. Greve, Stress magnitude and its temporal variation at Mt. Asama Volcano, Japan, from seismic anisotropy and GPS, *Earth Planet. Sci. Lett.*, **290**, doi:10.1016/j.epsl.2009.12.037, 2010.

Shimazaki, K. and Y. Zhao, Dislocation model for strain accumulation in a plate collision zone, *Earth Planet. Sci. Lett.*, **52**, 1091–1094, 2000.

Silver, P. G. and W. W. Chan, Shear wave splitting and subcontinental mantle deformation, *J. Geophys. Res.*, **96**, 16429–16454, 1991.

Sugaya, K., Y. Hiramatsu, M. Furumoto, and H. Katao, Coseismic change and recovery of scattering environment in the crust after the 1995 Hyogo-ken Nanbu earthquake, Japan, *Bull. Seismol. Soc. Am.*, **99**, 435–440, 2009.

The Japanese University Group of the Joint Seismic Observations at NKTZ, The Japanese University Joint Seismic Observations at the Niigaka-Kobe Tectonic Zone, *Bull. Earthq. Res. Inst., Univ. Tokyo*, **80**, 133–147, 2005 (in Japanese with English abstract).

Tsukuda, T., K. Sakai, S. Hashimoto, T. Haneda, and M. Kobayashi, Structual features of the precursory seismic gap and aftershock region of the 1990 southern Niigata earthquake of M5.4, *Bull. Earthq. Res. Inst., Univ. Tokyo*, **67**, 361–388, 1992 (in Japanese with English abstract).

Wessel, P. and W. H. F. Smith, New, improved version of Generic Mapping Tools released, *Eos Trans. AGU*, **79**, 579, 1998.

Yanagisawa, Y., I. Kobayashi, K. Takeuchi, M. Tateishi, K. Chihara, and H. Kato, Geological sheet map, scale 1:50,000, Ojiya, Geological Survey of Japan, Tsukuba, 1986.

Zatsepin, S. V. and S. Crampin, Modeling the compliance of crustal rock: I. response of shear-wave splitting to differential stress, *Geophys. J. Int.*, **129**, 477–494, 1997.

Y. Hiramatsu (e-mail: yoshizo@hakusan.s.kanazawa-u.ac.jp), K. Iwatsuki, S. Ueyama, T. Iidaka, and the Japanese University Group of the Joint Seismic Observations at NKTZ